

93-309



ОБЪЕДИНЕННЫЙ
ИНСТИТУТ
ЯДЕРНЫХ
ИССЛЕДОВАНИЙ
ДУБНА

E2-93-309

O.I.Piskounova

NOTION OF THE INCLUSIVE SPECTRA
AND CROSS SECTIONS OF B-MESON
PRODUCTION IN HADRONIC INTERACTIONS
OF HIGH ENERGIES

Submitted to «Ядерная физика»

1993

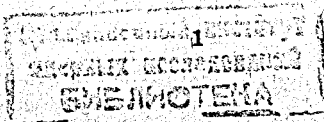
Introduction

It is generally accepted [1, 2] to present the heavy flavour hadroproduction in terms of diagrams of perturbation theory (PT) of QCD (see fig.1). Main subprocess is the $Q\bar{Q}$ pair formation in gluon-gluon fusion. Gluon momenta have to be not smaller than the mass of quark m_Q , thus the condition $\alpha_s(p_i^2) \ll 1$ is valid. But at the high energies the significant part of such subprocess will be contributed by the fusion of the soft hadronic components with the small part of proton momentum $x_1 \ll 10^{-2}$. Their momentum distributions cannot be calculated in the framework of PT QCD. Thus the calculated cross sections of heavy flavor quark hadroproduction will include the arbitrary corrections rising with energy because of semihard subprocesses. Another approach to this problem could be done from the side of peripheral models, which do not provide the accurate calculations of absolute values of cross sections, but use the phenomenological parameters. These models take into account the soft processes and give the description of multiple hadroproduction cross sections with the rise of energy. One of such models is Quark-Gluon String Model (QGSM) [3].

The multiple production cross sections are obtained in the framework of QGSM on the basis of supercritical pomeron phenomenology [4], where the main parameter, an intercept of Pomeron Regge trajectory: $\alpha_P(0) = 1,12 \pm 0,01$, was extracted at the approximation of total cross section dependence on energy. The stage of hadronisation is performed in QGSM as a rupture of cylinder pomeron strings into the chains of quark-antiquark pairs. These pairs form the secondary hadrons. Such obvious graphical approach allows one a) to account the dynamical alterations in the pattern of hadronic interactions when the energy increases and to obtain the energy dependence of cross sections in comparison to one observed experimentally at high energies; b) to account the condition of energy conservation for momentum distribution of produced hadrons; c) to account the connection between quark contents of interacting hadrons and secondary ones, which becomes to be important for particles produced in fragmentation regions of colliding hadrons.

1. The Scheme of B-Meson Production in QGSM

Let's consider in detail the description of multiple hadron distributions in the framework of QGSM. The main diagram of high energy hadron interaction is non-pomeron exchange diagram, shown in fig.2a). Such diagram with noninteracting



cylinder quark-gluon strings is the leading in $1/N_f$ expansion of QCD. On fig.2b)-2d) the examples of quark configurations on each side of cut cylinder are shown. The B^+ -mesons (see fig.2b),2c)) can be produced directly from the consistent quarks of interacting protons.

Differential cross section $x d\sigma/dx$ is saturated by partial cross sections of each n-pomeron cut configuration multiplied by fragmentation function

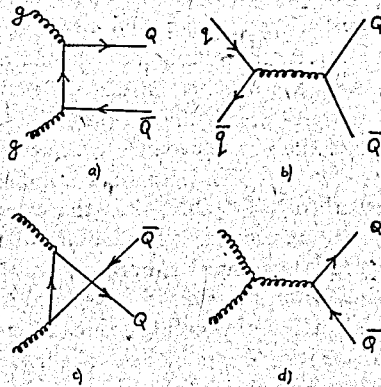


Fig.1. QCD diagrams for subprocesses with $b\bar{b}$ pair production.

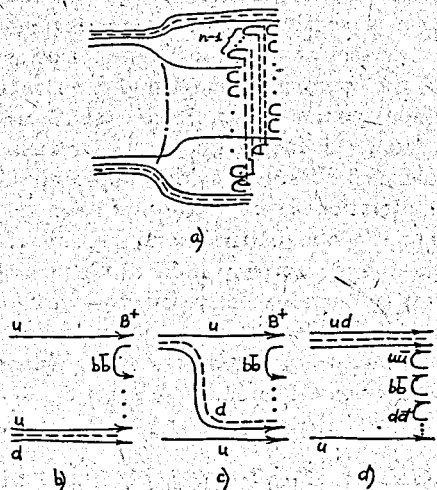


Fig.2. QGSM diagrams: a) n-pomeron exchange, b)-d) diagrams of B-meson production in the quark-antiquark chains.

$D_i(x/x_1)$ and quark distribution $f_i(x_1)$ which are converted on the part of energy x_1 :

$$f_1 = x \frac{d\sigma}{dx}(s, x) = \sum_{n=0}^{\infty} \sigma_N(s) \int_{x_{\pm}}^1 f_i(x_1) D_i(x_{\pm}/x_1) dx_1 \quad (1)$$

Here σ_0 is cross section of diffractive dissociation production, without any pomeron exchanges, and $x_{\pm} = 1/2(x + \sqrt{x^2 + x_1^2})$, $x_{\perp} = 2\sqrt{m_B^2 + p_{\perp}^2}/\sqrt{s}$. More detailed formulas could be found in the previous papers devoted to this model [5].

The quark structure function $f_i(x_1)$ has in QGSM the following asymptotics: $f_i(x_1) \sim x_1^{-\alpha_R(0)}$ at $x_1 \rightarrow 0$. The value of cross section $\sigma_{b\bar{b}}$ depends on physical parameters: $\alpha_P(0)$ - the intercept of Pomeron Regge-trajectory and $\alpha_T(0)$ - the intercept of Υ -meson trajectory. The estimation of $\alpha_P(0)$ was provided in [3] during the approximation of total cross section curve, and the value $\alpha_T(0)$ is restricted by the interval: $-16 \leq \alpha_T(0) \leq 0$. The shape of spectra of beauty particles at $x \rightarrow 1$ depends on $\alpha_T(0)$ because of the following asymptotics of fragmentation function: $D(x/x_1) \sim (1 - x/x_1)^{-\alpha_T(0) + const}$.

2. The Comparison of $b\bar{b}$ -Pair Production Cross Sections

Let us discuss hadroproduction cross sections for beauty quarks, presented in several papers [6] as the results of perturbative QCD calculations. The diagrams of considered basic subprocesses are shown on fig.1. The gluon fusion diagram (see fig.1a) is most important at high energies because the subprocesses passing through quark annihilation become to be of small probability. The values of heavy quark cross section depend on gluon structure function at small x_1 ($x_1 \ll 10^{-2}$).

The differential cross section dependence on the value of minimal transverse momentum p_{tmin} of B-meson observed in CDF experiment at $\sqrt{s} = 1.8$ TeV [7] was described in [8] due to PT QCD approach. Two curves are presented in this paper. First one is usual ISAJET program result, the second curve includes a corrected parametrisation of gluon structure function at $x_g \ll 10^{-2}$ having the following asymptotics: $1/x_g^{1.5}$. This variation allows to authors to get a good agreement between their results and experimental data points.

It should be noted that the asymptotics of multiparticle production cross sections at high energies in this case will be over the unitarized one given by supercritical pomeron theory. It will be better to use the phenomenological parametrisation of GSF of the following view: $1/x_g^{1.12}$.

The energy dependence of $\sigma_{b\bar{b}}$ obtained in the framework of QGSM [9] is presented in fig.3 a) in comparison with experimental values, given in literature. The curves for extremal values of intercept parameter: $\alpha_T(0) = 0$ and

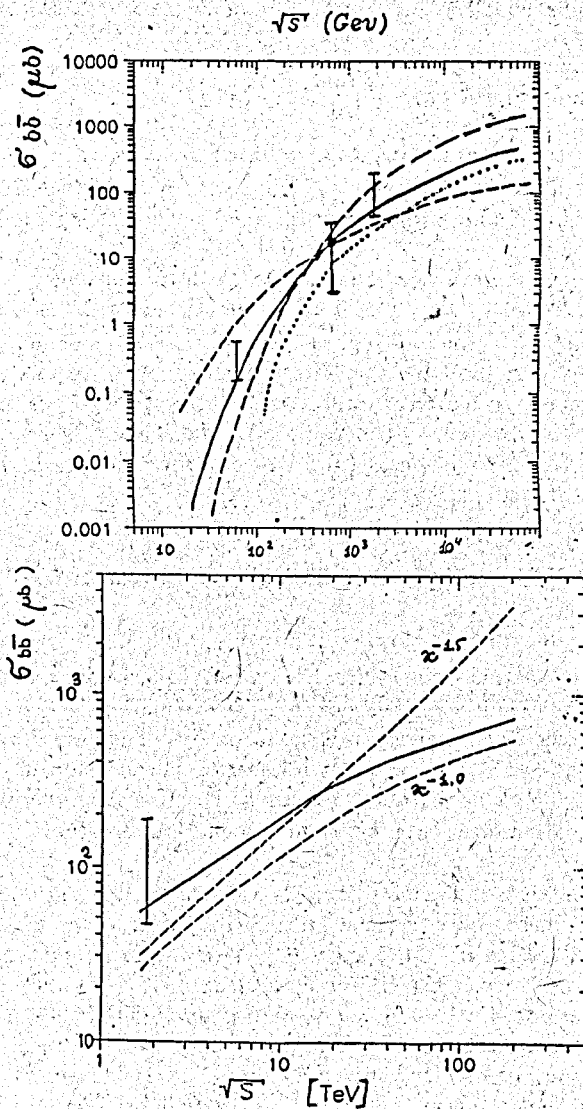


Fig.3. Cross sections of $b\bar{b}$ pair production at pp-interactions obtained in the experiments [10] and calculated in the framework of QGSM or in PYTHIA 5.3 program a) dashed lines correspond to extreme values of the $\alpha_T(0)$ parameter, a solid one is calculated at the optimal value: $\alpha_T(0)=-8$; cross sections obtained in PYTHIA program are represented in the dotted line, b) dashed lines depict the range of cross sections admissible in PYTHIA 5.3 at the various parametrizations of gluon structure function, the solid curve is obtained in optimal QGSM version.

$\alpha_T(0)=-16$ are shown by dashed lines. The limit of errors of cross section at $\sqrt{s}=1,8$ TeV was defined by approximation procedures. The experimental value of $\sigma_{b\bar{b}}(y|<1,0)$ was recalculated to full interval of rapidities with the help of QGSM dependence of x_F -spectra. The errors include an uncertainty, caused by the model dependence of differential cross sections on $\alpha_T(0)$. The best approximation to the energy dependence of production cross sections was achieved at $\alpha_T(0)=-8$ (the solid curve in fig.3 a). Cross sections obtained for certain energies at the generation of $b\bar{b}$ production events by PYTHIA 5.3 [11] (the dotted line in fig.3 a) are close to ones calculated in the framework of QGSM especially in high energy region. It is important, which set of structure functions for gluons and quarks was chosen. The modifications of those distributions at small x admissible into PYTHIA 5.3 cause to some corridor of cross sections at high energies [12] as it is shown in fig.3 b). The QGSM-curve with $\alpha_T(0)=-8$ goes in the middle, that is natural for given pomeron asymptotics of cross sections.

B^+ - and \bar{B}^0 -meson spectra, obtained in QGSM at the energy $\sqrt{s}=630$ GeV are compared in fig.4 with the resulting ones of PYTHIA 5.3. This QGSM spectra was calculated at the extremal value of $\alpha_T(0)=0$, that seems to be close to the result of PT QCD. It should be noted that there is no difference between leading B^+ - and unleading \bar{B}^0 -meson spectra obtained by PYTHIA 5.3. The first sort of mesons is produced directly with participation of valent quark of interacting protons. Differential cross sections of B^+ -mesons calculated at $\alpha_T(0)=-8$ are represented in fig.4 by dash-dotted line.

3. Summary

The comparison of B-meson hadroproduction spectra calculated in the framework of Quark Gluon String Model and generated by PYTHIA 5.3 program allowed us to reveal the discrepancies caused by nonperturbative effects. Both approaches predict the rise of cross section $\sigma_{b\bar{b}}$ at high energies: in QGSM it was achieved in the way of approximation of available experimental data with the choice of optimal value of $b\bar{b}$ -trajectory intercept $\alpha_T(0)=-8$, in PYTHIA results based on the perturbative calculations of main subprocesses the rising cross sections are conditioned in gluon structure function parametrization at very small x . Both models considered above give an approximately similar value of $\sigma_{b\bar{b}}=0.4$ mb at the energy of SSC. The discrepancy appears in x_F -distributions of B-mesons. QGSM-spectra obtained here are more soft than perturbatively calculated ones. No difference was observed in x_F -spectra of leading and unleading B-mesons generated by PYTHIA program. Such difference is due to the diverse fragmentations of valent quarks of protons into mesons containing b - and \bar{b} -quarks.

The author expresses her gratitude to A.B.Kaidalov, T.Sjöstrand and Yu.M.Shabelsky for useful discussions and to V.V.Glagolev and S.Tokar for the help in the working with PYTHIA 5.3 program.

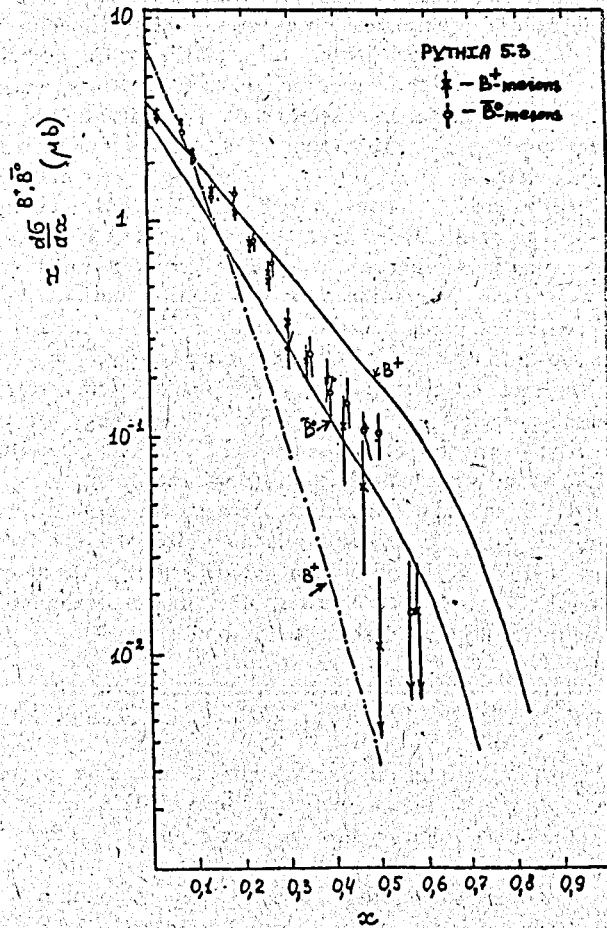


Fig.4. The comparison of B^+ and B^0 -meson spectra generated by PYTHIA 5.3 for the energy $\sqrt{s}=630$ GeV and calculated ones in the framework of QGSM: at $\alpha_T(0)=0$ (solid lines) and $\alpha_T(0)=-8$ (dashed-dotted one).

References

- [1] E.L.Berger and R.Meng, Phys.Rev.D **46**,169,1992.
- [2] J.Appel, Preprint FERMILAB-Pub-92/49,1992.

- [3] A.B.Kaidalov, Phys.Lett.**116B**,459,1982; A.B.Kaidalov, Phys.Lett.**116B**(1982)459; A.B.Kaidalov and K.A.Ter-Martirosyan, Phys.Lett.**117B**(1982)247.
- [4] J.L.Cardy, Nucl.Phys.**75B**,413,1974; A.Capella, J.Kaplan, Phys.Lett.**B52**,448,1974; M.S.Dubovikov and K.A.Ter-Martirosyan, Nucl.Phys.**B124**,163,1977.
- [5] A.B.Kaidalov and O.I.Piskounova, Zeit.für Phys.**C30**,145,1986; O.I.Piskounova, Preprint FIAN-140, Moscow, 1987
- [6] G.Altarelli et.al., Nucl.Phys.**B308**,724,1988; P.Nason, S.Dawson and R.K.Ellis, Nucl.Phys.**B327**(1989)49; J.C.Collins and R.K.Ellis, Preprint FERMILAB-Pub-91/22-T(1991).
- [7] CDF: A.Sansoni, Proceed.of the XXVI Rencontre de Moriond, 1991.
- [8] E.M.Levin, M.G.Ryskin, Yu.M.Shabelski and A.G.Shuvaev, DEZY 91-054.
- [9] O.I.Piskounova, Preprint FIAN-118, Moscow, 1990; A.De Rújula et.al., Preprint CERN-TH-6452, Geneva, 1992; L.Cifarelli, E.Eskut and Yu.Shabelski, Preprint EMCSC/ELN 92-02, 1992.
- [10] R422: L.Cifarelli, Nucl.Phys.Proceed.Supl.**1B**(1988)55; UA1: C.A.Albajar et.al., Phys.Lett. bf 256B(1991)121.
- [11] H.U.Bengtsson and T.Sjöstrand, Comput.Phys.Commun.**43**(1987)367.
- [12] J.R.Cudell et.al., Large Hadron Collider Workshop CERN 90-10, v.2, 164.

Received by Publishing Department
on August 10, 1993.